Polymer Journal (2018) 50:589–601
https://doi.org/10.1038/s41428-018-0052-8

FOCUS REVIEW

Advances in surface-coated single-walled carbon nanotubes as near-infrared photoluminescence emitters for single-particle tracking applications in biological environments

Zhenghong Gao[1]

Received: 30 January 2018 / Revised: 5 March 2018 / Accepted: 6 March 2018 / Published online: 24 April 2018

Abstract

Single-particle tracking (SPT) represents a powerful tool for revealing the single-molecule dynamics in a number of biological processes in live cells and biological tissue. Single-walled carbon nanotubes (SWCNTs) are promising photoluminescence emitters for SPT applications in various biological environments due to their characteristic large-aspect-ratio structures along with their bright and stable near-infrared (NIR) photoluminescence, which are invaluable for long-term video-rate imaging and tracking applications at the single-molecule level with high signal-to-noise ratios (SNRs). Recent advances in applying SWCNTs as NIR photoluminescence emitters have highlighted the understanding of brain tissue organization at the nanometer scale. In the first section, this review article summarizes the latest advances in different surface coatings commonly used for encapsulating SWCNT surfaces via molecular self-assembly in order to obtain surface-coated nanotubes with low cytotoxicity and minimal nonspecific interactions with live cells while maintaining their emission of bright photoluminescence to enable long-term photoluminescent imaging and tracking at the single-nanotube level in biological environments. The second section offers a comparison of different excitation strategies of (6,5) SWCNTs to determine the best excitation wavelength for efficient video-rate imaging and tracking of individual nanotubes in live brain tissue for up to tens of minutes without inducing unacceptable phototoxicity or temperature increases. Finally, this review showcases that, by utilizing the photoluminescence tracking of single nanotubes combined with super-resolution single-molecule localization microscopy technologies, it is practical to elucidate the ultrafine nanometer-scale organization of the brain extracellular space (ECS) and probe the local rheological properties of young rat brain with a subdiffraction optical resolution down to 50 nm at a subwavelength accuracy of ~40 nm. The findings primarily indicate the great diversity of the brain ECS and the inhomogeneous properties of the local viscosity in live brain tissue. Overall, because of their advantages of low cytotoxicity, bright photoluminescence, high SNRs (~25), and deep tissue penetration (~100 μm) for long-term video-rate imaging and tracking at the single-nanotube level under 845 nm excitation (K-momentum exciton–phonon sideband, KSB), phospholipid-polyethylene glycol-coated SWCNTs hold great potential as NIR photoluminescence emitters for single-particle tracking in biological environments, as exemplified here in live brain tissue, and may find extended applications in elucidating the fundamental roles of the brain ECS in various biological processes, such as sleep, memory, aging, brain tumor progression, and neurodegenerative disease development.

Introduction

Fluorescence imaging and tracking of biomolecules at the single-molecule level with single-particle tracking (SPT) techniques have yielded abundant knowledge that has enriched the understanding of single-molecule dynamics [1] and tissue organization at the nanometer scale in biology [2]. Single-molecule tracking (SMT) via SPT in living cellular environments is well established in cellular biology [3, 4], whereas the realistic challenge lies in imaging and tracking single molecules or particles within their native biological environments; an example is thick live brain

✉ Zhenghong Gao
zhenghong.gao@utsouthwestern.edu

[1] Department of Radiology, University of Texas Southwestern Medical Center, 5323 Harry Hines Boulevard, Dallas, TX 75390-8514, USA

tissue [5], which presents intense absorption and scattering of light and exhibits strong autofluorescence emitted from the natural fluorescent biomolecules inside the tissue under light illumination, significantly suppressing the key imaging parameter, the signal-to-noise ratio (SNR), and thus restricting the long-term observation of single-molecule or particle movement in the tissue. In this context, tracking single molecules or particles in intact biological tissue requires extraordinarily bright and stable fluorescence emitters to achieve long-term video-rate observations with continuously high SNRs at any given timescale. Additionally, the potential cytotoxicity and tissue inflammation induced by the fluorescence emitters must be minimized, and the photothermal tissue damage created by the light illumination delivered to the tissue to excite the fluorescence emitters (in many cases, high-energy power is needed) must be reduced.

Nanometer-sized emitters are attractive candidates for SPT applications in both live cells and tissues due to their excellent photostability during long-term observation compared to organic dyes and fluorescent proteins, which often suffer from a photobleached signal and allow only short-term imaging at the video rate [6]. During the past several years, investigations have focused on single-walled carbon nanotubes (SWCNTs), which are promising bright photoluminescence emitters for single-molecule and particle imaging and tracking because of their unique one-dimensional crystalline structures, high length-to-diameter ratios, characteristic diffusion behaviors, and near-infrared (NIR) photoluminescence. NIR photoluminescence falls in the optical window where biological tissues are most transparent, which is invaluable for obtaining high SNRs in deep tissue in many bioimaging applications.

This focused review aims to summarize the latest achievements in applying surface-coated SWCNTs as individual nanometer-sized emitters for single-particle imaging and tracking in thick live brain tissue and to showcase the essential findings on brain extracellular space (ECS) nanometer-scale organization unveiled by SPT combined with super-resolution imaging techniques. In brief, this review first focuses on comparing several SWCNT surface coatings in order to obtain nanotubes displaying low cytotoxicity while offering bright and stable photoluminescence to ensure single-nanotube imaging and tracking in biological environments. This review then presents an investigation of different excitation strategies at several wavelengths aimed to identify the optimal light wavelength for attaining high SNRs at the individual nanotube level in deep brain tissue with minimum phototoxicity. This review highlights the exploration of the brain ECS nanometer-scale organization via long-term video-rate tracking of the movement of individual SWCNTs for up to tens of minutes in live rat brain tissue. The findings suggest that phospholipid-polyethylene glycol (PLPEG)-coated SWCNTs are unique single-molecule emitters offering bright photoluminescence at the individual nanotube level within deep brain tissue while displaying low cytotoxicity and negligible inflammation in brain tissue upon administration of the SWCNTs at the dose required for SPT applications [7]. Laser beam excitation at 845 nm (K-momentum exciton–phonon sideband, KSB) results in consistently high SNRs, low phototoxicity, and reasonable temperature elevation compared to visible excitation at 568 nm resonance and upconversion excitation at 1064 nm; both laser beam excitations at 568 nm and 845 nm were previously proposed to be useful for bioimaging [8]. Excitation at 568 nm is in the visible light region and is mainly limited by high background fluorescence signals. Excitation at 1064 nm generates abundant thermal effects that dramatically increase the temperature inside the brain tissue, which induces phototoxicity and needs to be avoided [9]. Photoluminescence tracking of individual PLPEG-coated SWCNTs in acute live brain tissue slices was performed under continuous wave laser excitation at 845 nm. SWCNT trajectories of up to tens of minutes were recorded at a video rate of several tens of Hz. Quantitative analysis of the diffusion trajectories by using super-resolution single-molecule localization microscopy techniques revealed the nanometer-scale organization of the brain ECS in the live tissue with a resolution below 50 nm. These findings provide entirely new insights on the dynamic nanometer-scale dimensions and heterogeneous local viscosity of the ECS [10].

Superior over several widely used probes, such as organic dyes [6], proteins [6], and spherical quantum dots (QDs) [11], SWCNTs have two characteristic dimensions that define their unique diffusion properties; their small diameter (few nanometers) enables remarkable accessibility in confined environments. The combination of their small diameter, long length, length-dependent structural rigidity, and stable NIR photoluminescence (Fig. 1a, b) makes SWCNTs suitable for long-term video-rate imaging and tracking at the single-molecule or particle level (Fig. 1a) [12]. Tracking single SWCNTs in live brain tissue allowed accessing and quantitatively characterizing the nanometer-scale organization of the brain ECS within its native environment [10]. These findings have provided new knowledge promoting our understanding of the biophysical properties and functions of the ECS at the nanometer scale, suggesting that surface-coated SWCNTs are indeed promising nanometer-sized NIR emitters suitable for long-term photoluminescence tracking applications in complex biological environments. Surface-coated SWCNTs may be applied for probing brain tissue properties in both healthy and diseased, e.g., brain tumors and degenerative diseases, brain models. Herein, the advances in surface coating

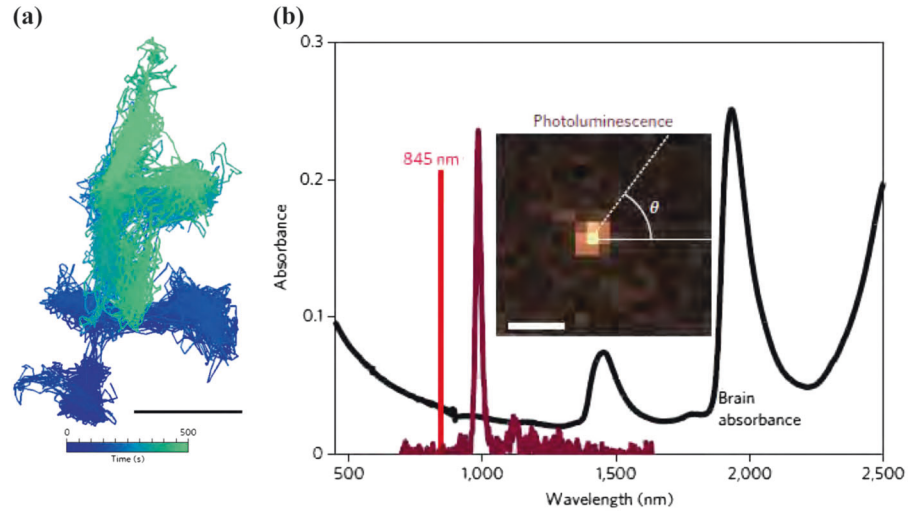

Fig. 1 Photoluminescence tracking of single SWCNTs in live ECS brain tissue. **a** Color-coded trajectory of a single SWCNT diffusing in live brain tissue. Scale bars, 1 μm. **b** Absorbance spectrum of a 1 mm thick brain slice (black) and photoluminescence spectrum of a single (6,5) SWCNT in the ECS (purple) under 845 nm laser excitation (red). Inset, photoluminescence image of a (6,5) SWCNT recorded in the ECS with an orientation θ. Adopted from ref. [10], Copyright© 2016, Springer Nature

identification, excitation strategies, and single-nanotube tracking inside the ECS in live brain tissue are described.

Identification of surface coatings for SWCNTs suitable for single-particle tracking in biological environments

SWCNTs are excellent photoluminescence emitters because of their high brightness and the photostability of their NIR-range photoluminescence [13, 14]. High-SNR microscopic imaging of assembled SWCNTs has been achieved in live cells and animals [15, 16]; however, photoluminescence detection at the single-nanotube level has been a great challenge with respect to the complexity of biological environments, for example, live brain tissue, and requires that SWCNTs possess good biocompatibility, low toxicity, and bright and stable photoluminescence to ensure long-time course imaging and tracking while maintaining high SNRs. Although several types of surface coating-encapsulated SWCNTs have been imaged and tracked at the single-nanotube level both at the cellular plasma membrane and in the intracellular area of live cell cultures [17, 18], as well as in the ECS of three-dimensional tumor spheroids [19], the impact of surface coatings on the non-specific interactions between SWCNTs and living cells is not fully understood yet. For SPT applications in thick tissue, the accessibility of SWCNTs in confined biological regions within the tissue is predominately affected by the sticky interactions of the nanotubes with tissue, similar to other nanomedicine systems [20]. This stickiness mainly originates from the nonspecific interactions of SWCNTs with biomolecules inside the tissue, e.g., electrostatic, Coulomb, or van der Waals interactions, as opposed to specific and controlled nanotube–biomolecule interactions [21]. It is important to note that the nonspecific interactions may partly be responsible for the cytotoxicity of nanoparticles [22, 23]. Therefore, minimized nonspecific interactions largely reduce the sticking of SWCNTs to cells within the tissue, thus allowing the nanotubes to diffuse and explore the confined structural spaces/domains for a long period of observation time. Additionally, SWCNT photoluminescence is ultrasensitive to attached surface coating molecules [24], dependent on the length of such molecues [25, 26], and related to the defective states in their backbones [27, 28] and the local chemical environments [29, 30]. In this context, it is critical to form biocompatible SWCNTs with a surface coating that ensures minimum nonspecific interactions with living cells and tissues while maintaining the nanotubes' photoluminescence brightness during long-term video-rate observations.

A number of surfactants and polymers known to endow surface-coated SWCNTs with good photoluminescence have been widely used for coating and stabilizing nanotubes in aqueous suspensions. Recently, several commonly used polymer coatings were selected and evaluated for encapsulating SWCNTs via molecular self-assembly on nanotube surfaces (Fig. 2); these coatings have the potential to maintain the brightness of photoluminescence while displaying low cytotoxicity and minimizing nonspecific interactions with cells and tissues. These studies aimed to determine the most suitable coating agent that displays low nonspecific interactions and ensures bright SWCNT photoluminescence for imaging with high SNRs at the single-nanotube level in biological environments. Several small molecular weight surfactants including sodium dodecylbenzene sulfonate or bile salts (NaDOC) are known to yield SWCNTs with bright photoluminescence in aqueous environments [31, 14, 30]; however, their uses in cellular imaging are not likely favored because these surfactants significantly interrupt the organization of cellular membranes [32, 33]. It is also noted that small peptide [34]- and nucleic acid [18]-coated carbon nanotubes are less stable

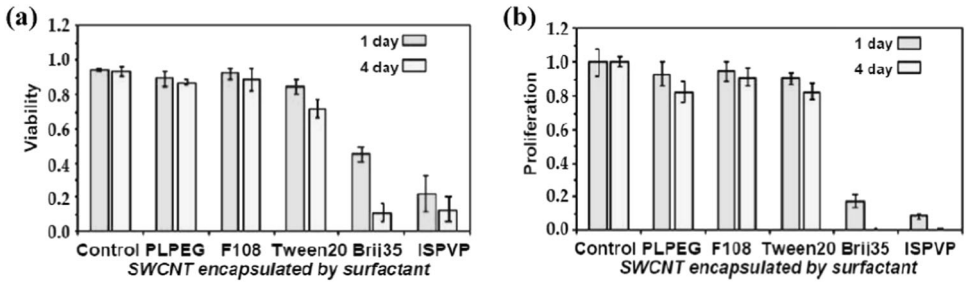

Fig. 2 Biocompatibility of different surface-coated SWCNTs in live cells. Comparisons of cellular **a** viability and **b** proliferation of COS7 cells incubated with PLPEG-, F108-, Tween20-, Brij35-, and ISPVP-coated SWCNTs for 1 day and 4 days. Starting concentration of COS7 cells: 1×10^5 cells/mL; SWCNTs: 1 μg/mL; cells cultured at 37 °C with 5% CO_2. Three independent experiments were performed to obtain standard variations. Cell viability was evaluated using trypan blue dye staining. Adopted from ref. [7], distributed under the Creative Commons Attribution License

than many polymers that possess larger molecular weights and flexible conformations [35]. To identify the best polymer coating for SWCNTs in SPT applications, a panel of polymer coatings previously used for encapsulating SWCNTs for applications in bioimaging and/or drug delivery were selected and examined. These polymers include PLPEG [15, 36], Pluronic (F108) [37], Tween20 [38], Brij35 [39], and in situ polymerized (poly)vinyl pyrrolidone (ISPVP) [24] and are potentially biocompatible coating agents that have been used to stabilize SWCNTs (Fig. 2) for various biomedical applications. In experiments, surface-coated SWCNTs were incubated with COS7 cells for 1 day and 4 days at a dose of 1 μg/mL, equivalent to that required for SPT applications, and cell viability and proliferation were examined. After 1 day of incubation, PLPEG-, F108-, and Tween20-coated SWCNTs showed no apparent impact on cell proliferation and viability (Fig. 2a, b), and these results were very similar to those of control cells without SWCNT administration. Only a small number of cells were found to be unhealthy or deceased after 4 days of incubation; COS7 cells maintained their normal proliferation rate, which was similar to that of the control cells (Fig. 2b). These results suggest that PLPEG, F108, and Tween20 might be promising candidates for coating SWCNT surfaces for SPT applications because these polymer-coated nanotubes may have low cellular toxicity over the exposure time and at dose level suitable for SPT. In contrast, Brij35- and ISPVP-coated SWCNTs dramatically reduced the cell proliferation rate, and a large portion of cells was found to be unhealthy or deceased after only 1 day of incubation (Fig. 2a); more dead cells were found after 4 days of incubation (Fig. 2b). Brij35- and ISPVP-coated SWCNTs may have also impacted the attachment of cells onto the culture dishes, which caused cell detachment from the culture dish substrate during incubation or washing in sample preparation. These results suggest that Brij35- and ISPVP-coated SWCNTs may eventually cause cellular toxicity even at very low doses within a short incubation time, and the utilization of these polymer-coated SWCNTs for imaging and tracking in live cells and tissues may need to be avoided. In this case, the potential cytotoxicity was evaluated at a very low dose suitable only for SPT applications; high-dose exposure was clearly beyond the scope of the applications. As a matter of fact, the toxicity of SWCNTs is complicated and related to many aspects; a more detailed review regarding this topic can be found in a recent article by Gao et al. [40].

The nonspecific interactions of PLPEG-, F108-, and Tween20-coated SWCNTs with live cells were assessed by using photoluminescence imaging (Fig. 3) to provide direct images of SWCNTs attached to cells [7]. In the experiments, SWCNTs were incubated with COS7 cells for 1 day, and the cells were washed with culture media to remove free nanotubes in the culture. The immobilized SWCNTs on live cells that resulted from nonspecific interactions were counted, which prevented diffusion of the nanotubes from the cells to the culture medium after washing. A wide-field fluorescence microscope capable of detecting single SWCNTs in cell cultures and tissue was employed to image the nanotubes. (6,5) SWCNTs were intentionally selected for the study because their favored NIR emission falls within the transparent range of tissue. Excitation was performed at 845 nm at the photon sideband of the (6,5) nanotubes with a continuous wave laser, and photoluminescence at 968 nm was collected by a highly sensitive camera equipped with a microscope setup. With this imaging configuration, both excitation and emission were perfectly aligned within the window of biological tissue transparency, which helps in detecting SWCNTs located deep within tissue and reduces the tissue phototoxicity potentially induced by the excitation and emission light. The experimental results indicate that PLPEG- and F108-coated SWCNTs have significantly fewer interactions with cells, different from nanotubes coated with Tween20. Many Tween20-coated nanotubes were found interacting with cells, as indicated by the bright photoluminescent objects in

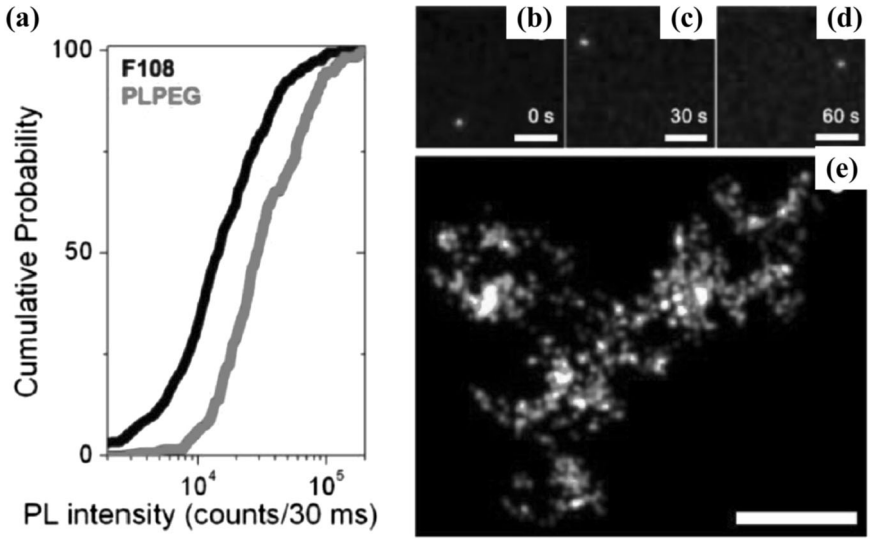

Fig. 3 Photoluminescence imaging and tracking of individual SWCNTs. **a** Cumulative distribution of the photoluminescence intensities from 162 (resp. 256) individual PLPEG (resp. F108)-coated SWCNTs in biological media (DMEM). **b–d** Single PLPEG-coated SWCNT tracking in 1.5% agarose gels: three frames, separated by 30 s, of an ~1 min movie acquired at 33 Hz is displayed, revealing the SWCNT trajectory within the gel. **e** Super-resolved map of the gel structure reconstructed from the collection of 2096 super-localized nanotube positions while the nanotube was diffusing. Scale bar: 5 µm. Adopted from ref. [7], distributed under the Creative Commons Attribution License

these images. It is notable that certain small SWCNT bundles may also be present in these images, and these experiments were not designed to point out whether some nanotubes may be released into the media or internalized into cells after a certain time. These observations suggest that PLPEG- and F108-coated SWCNTs have minor nonspecific interactions with live cells, which are in agreement with previous discoveries in vivo [41, 42] in which PLPEG-coated SWCNTs showed prolonged circulation in blood and F108-coated nanotubes exhibited deceased lung fibrosis potential. Taken together, these findings indicate that SWCNTs have the potential to be applied in SPT applications because of their minimized nonspecific interactions, which decrease the possibility of the nanotubes sticking to live cells, enable great accessibility of the nanotubes inside the tissue and consequently allow long-term nanotube diffusion to fully explore confined environments.

The photoluminescence brightness was quantitatively examined for PLPEG- and F108-coated SWCNTs at the single-nanotube level in cell culture media in the presence of serum required for cell growth (Fig. 3a). The results suggested that PLPEG-coated SWCNTs were significantly brighter than nanotubes coated with F108 (Fig. 3a). The median photoluminescence brightness of PLPEG-coated SWCNTs was approximately twofold greater than that of F108-coated nanotubes (Fig. 3a) in cell culture media. The photoluminescence of SWCNTs is directly related to their surface coating type, stability, density, and so on. The stability of surface-coated SWCNTs in biological environments is an essential factor accounting for the nonspecific interactions with cell membranes. It has been reported previously that F108 molecules could detach from the surface of SWCNTs in biological environments, particularly in the presence of serum [37, 40]. The interactions between F108 and the nanotube surface are not sufficient to compete with the interactions between the nanotube surface and the proteins contained in serum, which can attach to nanotube surface and replace F108; serum proteins are known to reduce nanotube photoluminescence [43]. PLPEG-coated SWCNTs are relatively stable in the presence of serum [41] and offer bright photoluminescence due to the robust interactions between PLPEG and SWCNTs. No similar detachment and replacement for PLPEG-coated SWCNTs was suggested by these observations. PLPEG interacts with the SWCNT surface mainly via molecular self-assembly through hydrophobic interactions [44]. The PL lipid head is hydrophobic and attaches to the SWCNT backbone via the self-assembly driven by the intramolecular interactions that best preserve the integrity of the nanotube's π-network, which is crucial for maintaining bright photoluminescence. The PEG tail as a long hydrophilic chain with good structural flexibility; PEG expands in water and functions to suspend and stabilize nanotubes in aqueous environments. Coating PLPEG on carbon nanotubes via molecular self-assembly may lead to unique structural patterns on the nanotube surface that are dependent on the nanotube chirality, and PEG length, density, and conformation. The formed complexes were remarkably stable

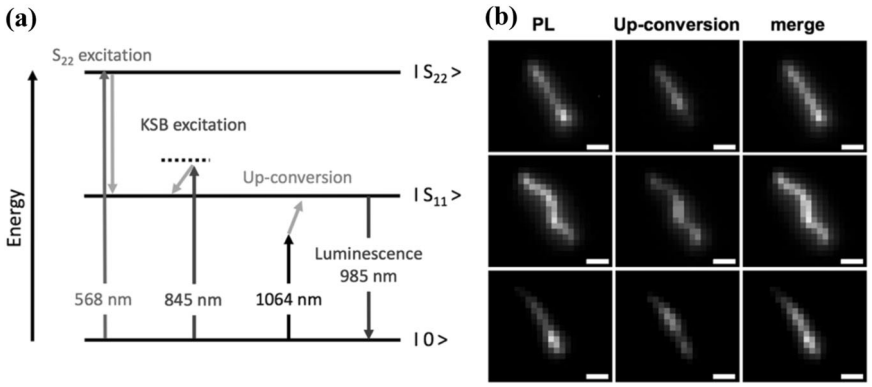

Fig. 4 Three excitation strategies for (6,5) SWCNTs. **a** Diagram showing the different excitation strategies for obtaining luminescent (6,5) SWCNTs. **b** Luminescence images of micrometer-long (6,5) nanotubes suspended in NaDOC using 568 nm photoexcitation (0.2 kW/cm^2) or 1064 nm upconversion (3.2 kW/cm^2) with cw lasers in a wide-field configuration. Integration time: 100 ms. Scale bar = 1 µm. Adopted from ref. [9], Copyright© 2018, American Chemical Society

depending on the curvature of the nanotube surface [45]. A high-density coating of high molecular weight PEG or branched and star-shaped PEG on the SWCNT surface has been suggested to improve the stability and performance in vivo [46, 47]. In biological environments, PEG molecules form a soft antifouling shell around nanotubes and prevent nanotubes from directly interacting with biomolecules via nonspecific interactions [48]. Different types of PEG and polymers were recently discovered to endow carbon nanotubes with distinct molecular recognition properties [49]. A similar PEG coating approach has been applied for developing drug delivery systems with minimized potential to form protein corona—nonspecific absorption of serum proteins on the nanoparticle surface [50, 51]. The PLPEG-coated SWCNTs showed bright photoluminescence and are promising for SPT applications.

To test whether SWCNTs are capable of moving/diffusing in biological environments, PLPEG-coated SWCNTs were embedded in 1.5% agarose gel, an artificial mimic of the biological environment that was previously used to investigate the Brownian diffusion of single nanotubes in crowded environments [12]. Photoluminescence tracking of diffusing individual nanotubes within the gel with high-SNR imaging for a period of up to tens of minutes at a video rate of 33 Hz was achieved (Fig. 3b); this tracking was a direct result of the bright and stable NIR photoluminescence emitted of the PLPEG-coated SWCNTs [7]. The position of SWCNTs at each time point was localized with an accuracy of ~50 nm by using super-resolution single-molecule localization microscopy techniques (Fig. 3b). The super-resolved map of the porous gel structure was then rebuilt by successively linking the super-localized nanotube positions (Fig. 3b). This gave a single-nanotube tracking application with a 50 nm subdiffraction resolution for the detection of nanometer-scale gel dimensions. In this way, it is feasible to visualize the ultrafine structure and dynamic organization of a gel at the nanometer scale. These findings indicate that PLPEG-coated SWCNTs are nanometer-scale emitters with bright and stable NIR photoluminescence and negligible cytotoxicity and nonspecific interactions with cells. They are suitable single-molecule labels/probes and applicable as SPT probes to explore complex biological environments, such as live brain tissue.

Comparison of SWCNT excitation strategies for an optimized wavelength to attain a high SNR for long-term video-rate imaging and tracking in biological environments

SWCNTs with bright photoluminescence are novel nanometer-sized emitters that owing to their unique optical properties, enable single-molecule or particle-level detection in biological environments [52, 10]. Recent advances have shown the successful tracking of single nanotubes with negligible photobleaching in live cells [18] and tissue [10]. Several excitation strategies at distinct wavelengths can be used to excite electrons in SWCNTs from the ground state to the excited state. For video-rate imaging of individual SWCNTs within biological tissue, it is necessary to use an excitation strategy that is most suitable for detecting single nanotubes while maintaining a high SNR and minimizing potential photon-induced damage and thermal-induced temperature increases in biological tissue. When detecting SWCNTs at the single-molecule level in biological tissue, the photoluminescence signal of a single nanotube is quite low and can be easily masked by tissue autofluorescence and scattering [53]. In this context, SWCNTs need to be wisely chosen by taking into account the nanotube chirality [54], absorption, and emission to maximize the ability to maintain a high SNR over a long observation timescale. (6,5) SWCNTs were a focus of consideration because of their bright and stable photoluminescence for long-term

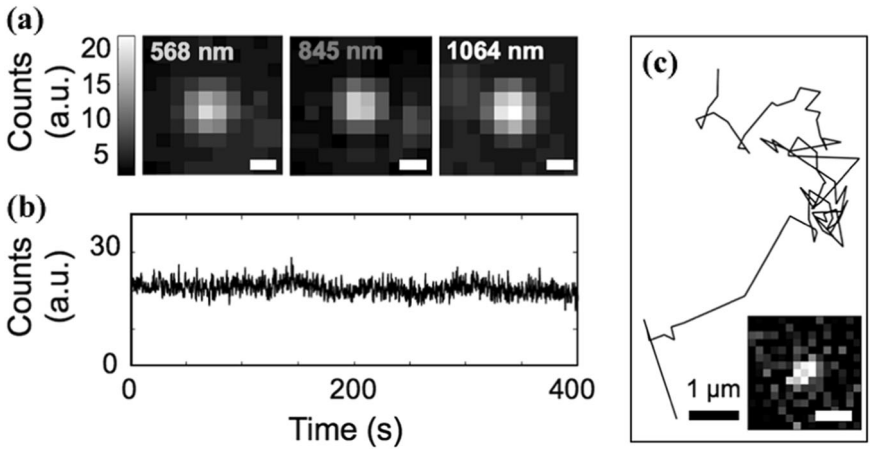

Fig. 5 Photoluminescence imaging and tracking of individual PLPEG-coated (6,5) SWCNTs under different excitation wavelengths. **a** Luminescence images of a single (6,5) excited SWCNT exciting using a 568, 845, or 1064 nm cw laser in a wide-field configuration (from left to right, respectively). Laser intensity: 0.4 kW/cm^2 (568 nm), 1.6 kW/cm^2 (845 nm), and 6.4 kW/cm^2 (1064 nm). Integration time: 100 ms. Scale bar = 500 nm. **b** UCL signal of a single (6,5) PLPEG-SWCNT recorded over 400 s. Laser intensity: 6.4 kW/cm^2; 100 ms integration time per point. **c** Single-nanotube tracking showing the 2D trajectory of a single (6,5) SWCNT diffusing in cell culture medium (DMEM) imaged by UCL using a 1064 nm cw laser (30 ms per frame). Laser intensity: 3.2 kW/cm^2. Adopted from ref. [9], Copyright© 2018, American Chemical Society

single-nanotube tracking without photobleaching [10], along with their favorable NIR absorption [55] and emission [56] for deep tissue penetration in live cells and brain tissue. The aim was to determine an optimized excitation strategy by comparing the available excitation options to facilitate long-term video-rate imaging/tracking of photoluminescent (6,5) SWCNTs at the single-nanotube level in biological tissues with a high SNR. To this aim, SWCNT absorption and photoluminescence properties were taken into account together with some critical tissue features including light absorption and scattering at different wavelengths, where excitation can be performed. The impacts of light scattering and absorption were considered in this study [9] because these factors are the initial causes of tissue autofluorescence and temperature increases and may eventually affect the SNR and induce tissue phototoxicity.

The photoluminescence efficiencies of single (6,5) SWCNTs were compared under excitation at three different wavelengths, corresponding to the second-order excitonic transition [55], K-momentum exciton–phonon sideband [57], and upconversion (Fig. 4a, b) [8, 9]. The second-order excitonic transition S22 is frequently used to excite SWCNTs because of the broad resonance absorption cross-section at 568 nm of (6,5) nanotubes [55]. The K-momentum exciton–phonon sideband, denoted KSB, has been suggested to offer better photoluminescence stability and deep tissue penetration; the wavelength is at 845 nm for (6,5) nanotubes [10]. The upconversion photoluminescence (UCL) of (6,5) SWCNTs was recently discovered, and the excitation energy is usually provided by a pulsed NIR laser at 1064 nm at an energy value smaller than the first-order excitonic transition S11 [8]. The upconversion photoluminescence holds great promise for in vivo bioimaging due to its potential for deep tissue imaging. These three choices were compared for the excitation of photoluminescent (6,5) SWCNTs at the single-nanotube level to determine the best excitation wavelength for achieving high SNRs.

Individual (6,5) PLPEG-coated SWCNTs immobilized in a polymer layer coated on a thin glass substrate were imaged by using a homemade wide-field fluorescence microscope equipped with circularly polarized laser beams capable of exciting carbon nanotubes at 568 nm for resonant S22 excitation, 845 nm for resonant KSB excitation, or 1064 nm for UCL (Fig. 5a). Photoluminescent (6,5) SWCNTs were successfully imaged at a video rate (30 ms per frame) at all three excitation wavelengths in cell culture media, and the trajectory (Fig. 5c) was recorded and rebuilt for up to several minutes due to the excellent stability of the photoluminescence (Fig. 5b).

The photoluminescence efficiency of the individual (6,5) PLPEG-coated SWCNTs at three excitation wavelengths was first quantified by analyzing the mean photoluminescence count rate per pixel. S22 excitation gave the highest count rate among the three excitations strategies, and the mean value was up to four times more efficient than that of KSB excitation and more than ten times more efficient than that of upconversion excitation at 1064 nm. The relative efficiencies normalized by the value obtained at 1064 nm were 17.5 ± 1.2, 4.6 ± 0.3, and 1.0 ± 0.2 for 568, 845, and 1064 nm, respectively [9].

Table 1 Light absorption and scattering in the rat brain cortex

λ (nm)	$\mu_{a,oxy}$ (cm^{-1})	$\mu_{a,deoxy}$ (cm^{-1})	$\mu_{a,water}$ (cm^{-1})	$\mu_{a,fat}$ (cm^{-1})	μ_a (cm^{-1})	μ_s total (cm^{-1})
568	300	300	6.5×10^{-4}	6.5×10^{-2}	9	21.5
845	5	3	5×10^{-2}	6.5×10^{-2}	0.17	11.7
1064	3	0.5	0.8×10^{-1}	4×10^{-1}	0.7	8.7

Note: The terms $\mu_{a,oxy}$ and $\mu_{a,deoxy}$ represent absorption by oxygenated and deoxygenated HGb, respectively. $\mu_{a,water}$ absorption by water, $\mu_{a,fat}$ absorption by lipids. Adopted from ref. [9], Copyright© 2018, American Chemical Society

To perform single-nanotube detection in live tissue, it is important to include the impacts of tissue scattering and absorption that eventually result in tissue autofluorescence and temperature elevation. The amounts of light absorption (μa) and scattering (μs) per unit length at these three excitation wavelengths were calculated using theoretical models (Table 1) [9, 58]. The simulated results are shown in Table 1. The results showed that the tissue scattering dramatically decreased with the increase in the light wavelength, while absorption was lowest at 845 nm. Excitation at 1064 nm ensures minimum tissue scattering and absorption by blood but is not as efficient as excitation at the other two wavelengths because water absorbs 1064 nm light more efficiently than 568 nm and 845 nm light in this range [9]. Tissue autofluorescence is another important factor that needs to be included because of its large impact on the SNR. In general, the level of autofluorescence decreases as the wavelength increases [27]. In this sense, 1064 nm excitation generates less autofluorescence than 568 nm and 845 nm excitation.

Next, the SNRs of single PLPEG-coated SWCNTs in brain tissue were compared (Fig. 6a–f). SWCNTs were injected into the lateral cerebroventricle of rat brain. This injection method was used for directly delivering SWCNTs into the brain and avoiding blood exposure; with this method, tissue inflammation was minimized, and the native tissue architecture was mostly well preserved [2]. Acute brain tissue slices with a thickness of ~100 μm were prepared after killing animals and fixed for imaging on our NIR single-nanotube microscope. In the fixed brain tissue, most SWCNTs were found to be located in the brain ECS (Fig. 6b). The signal-to-background ratios were then obtained at three excitation wavelengths (Fig. 6c–e); the mean values were 2.5, 0.3, and 0.1 for 1064 nm, 845 nm, and 568 nm, respectively (Fig. 6f). The excitation at 1064 nm offered SNRs of ~25, nearly identical to that at 845 nm and significantly better than the SNRs of ~5 at 568 nm excitation [9]. It is clear that excitation at 1064 nm and 845 nm yields a good SNR, which is the key parameter for efficient single-nanotube detection in biological environments.

Illuminating biological tissue with light generates a photothermal effect and increases the temperature inside the tissue, which may cause photon-induced damage to cells within the tissue. With a simple simulation mimicking the imaging setup and experimental conditions and at the laser energies needed for collecting the same level of photoluminescence at 568, 845, and 1064 nm excitation, it was found that 1064 nm light caused a temperature increase of up to 15 K, which was much higher than the 8 and 0.8 K increases at 568 nm and 845 nm excitation, respectively (Fig. 7) [9]. These results suggest that 1064 nm excitation may not be suitable for individual nanotube imaging and tracking in biological tissue due to the strong absorption of water at this wavelength, which efficiently induces a strong photothermal effect and heats up the biological tissue. Excitation at 845 nm induced a lower temperature increase in brain tissue than excitation at 1064 nm, indicating that 845 nm is more suitable for exciting individual (6,5) PLPEG-coated SWCNTs in brain tissue.

After systematically evaluating the photoluminescence efficiencies of individual (6,5) PLPEG-coated SWCNTs in aqueous media at three different excitation wavelengths and considering the impact of light absorption, scattering, autofluorescence, and temperature elevation inside brain tissue, it was found that excitation at the K-momentum exciton–phonon sideband at 845 nm is the preferred wavelength for video-rate imaging of single (6,5) PLPEG-coated SWCNTs in biological tissue because 845 nm excitation offered good SNRs and minimum phototoxicity to tissue.

Photoluminescence tracking of individual SWCNTs in live brain tissue to reveal the brain ECS nanometer-scale organization

The brain ECS is the fundamental biological structure essential for maintaining normal brain functions and activities. The ECS provides a dynamic biological space for the transition of neurotransmitters, nutrients, and other signaling molecules inside the brain [59–61]. The ECS exists in the brain as the microenvironment for cellular communication [62] and brain waste clearance [63]. The ECS organization undergoes dynamic changes during many biological processes, including sleep [63], memory, and aging [64], and probably plays key roles in neurodegenerative disease development [65] and tumor progression [66]. However, its ultrafine structure and low-dimensional organization, particularly in live brain tissue, are very poorly understood mainly due to the lack of a powerful approach for imaging them in their native environment. Many previous studies have used electron microscopy to study the brain tissue ultrafine structure and high-resolution orgnization [67]. In such methods, brain tissue needs to be treated with harsh chemicals in order to fix it and imaged at

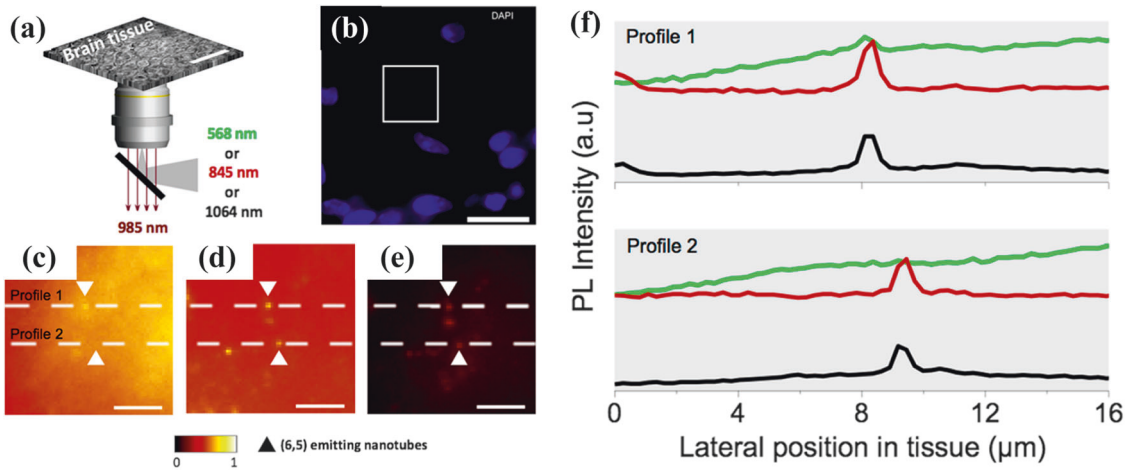

Fig. 6 Comparison of the photoluminescence signals of PLPEG-coated (6,5) SWCNTs under laser excitation at 568, 845, and 1064 nm. **a** Schematics of the experimental setup used to image single (6,5) SWCNTs in a brain slice. **b** DAPI staining of the brain slice was used to identify cell nuclei. The highlighted square depicts the region shown in **c**–**e**, where single SWCNTs are imaged. Scale bar = 20 μm. **c**–**e** Single (6,5) SWCNTs imaged 50 μm inside a brain slice (arrows) using laser excitation at 568 nm (**c**), 845 nm (**d**), or 1064 nm (**e**) in a wide-field configuration. Scale bar = 5 μm. The laser intensities were adjusted to obtain comparable SWCNT luminescence signals. **f** Signal obtained from the profiles indicated in **c**–**e** (green for 568 nm, red for 845 nm, and black for 1064 nm excitation). Adopted from ref. [9], Copyright© 2018, American Chemical Society

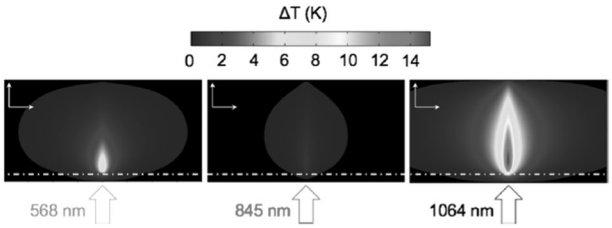

Fig. 7 Simulation of the temperature elevation of brain tissue. Laser excitation was set at 568, 845, or 1064 nm, and excitation intensities were set to excite an individual (6,5) SWCNT situated 50 μm inside the tissue and displaying identical luminescence. The laser intensities were 0.23 kW/cm^2 for 568 nm excitation, 0.80 kW/cm^2 for 845 nm excitation, and 3.64 kW/cm^2 for 1064 nm excitation, which correspond to 0.20, 0.75, and 3.47 kW/cm^2, respectively, at the nanotube to correct for tissue absorbance. The dotted line indicates the interface between the coverslip and the tissue. Excitation beams were incident from the bottom, as indicated by the arrows. Vertical and horizontal scale bars: 500 μm. Adopted from ref. [9], Copyright© 2018, American Chemical Society

ultra-low temperatures with cryotechnology [67], which is known to cause tissue damage, distortion, and deformation. These are obviously irreversible alterations to the native tissue architecture and organization [68]. To study the ultrafine structure and low-dimensional organization of the brain at high resolution requires the use of live brain tissue with its native architecture as well as other important physiological features perfectly preserved. For this purpose, acute brain tissue slices were prepared and provided with the necessary materials during imaging to maintain the living tissue ex vivo for ~1 h. Video-rate fluorescence tracking of single particles in live brain tissue can be useful for analyzing the successive positions of single emitters diffusing inside the tissue with super-resolution techniques with an imaging resolution below the diffraction limit [6, 52]. Long-term tracking in deep tissue helps record the full dynamic history of single emitters' diffusion in their native environment. Moreover, a slow diffusion rate modulated by the intrinsic structure of the nanoparticles is favored for efficient video-rate recording of the movement trajectory [12]. SWCNTs meet all these requirements because of their characteristic structures, high length-to-diameter ratios, and length-dependent rigidity, as well as their bright and stable NIR photoluminescence [13].

PLPEG-coated SWCNTs were injected into the lateral cerebroventricles of live rats. As suggested by the above-mentioned investigations, these nanotubes have low toxicity and bright luminescence compared to other nanotubes with different coatings [7, 15]. The delivery approach resulted in minimal inflammation in tissue after nanotube injection. Young rats with injected SWCNTs were killed approximately half an hour post injection. Acute brain tissue slices were prepared and imaged on an NIR single-nanotube microscope at 845 nm excitation with a peak emission at 986 nm of the (6,5) nanotubes (Fig. 8a). In this configuration, both excitation and emission are perfectly aligned in the optical region, where tissue is most transparent and are optimal for attaining a high SNR, an excellent penetration depth, and minimized phototoxicity.

Photoluminescent (6,5) SWCNTs were found within a thick tissue layer down to 100 μm from the tissue surface, and time-lapse images of single-nanotube diffusion were recorded for a time period of up to tens of minutes due to the good photoluminescence stability under 845 nm excitation

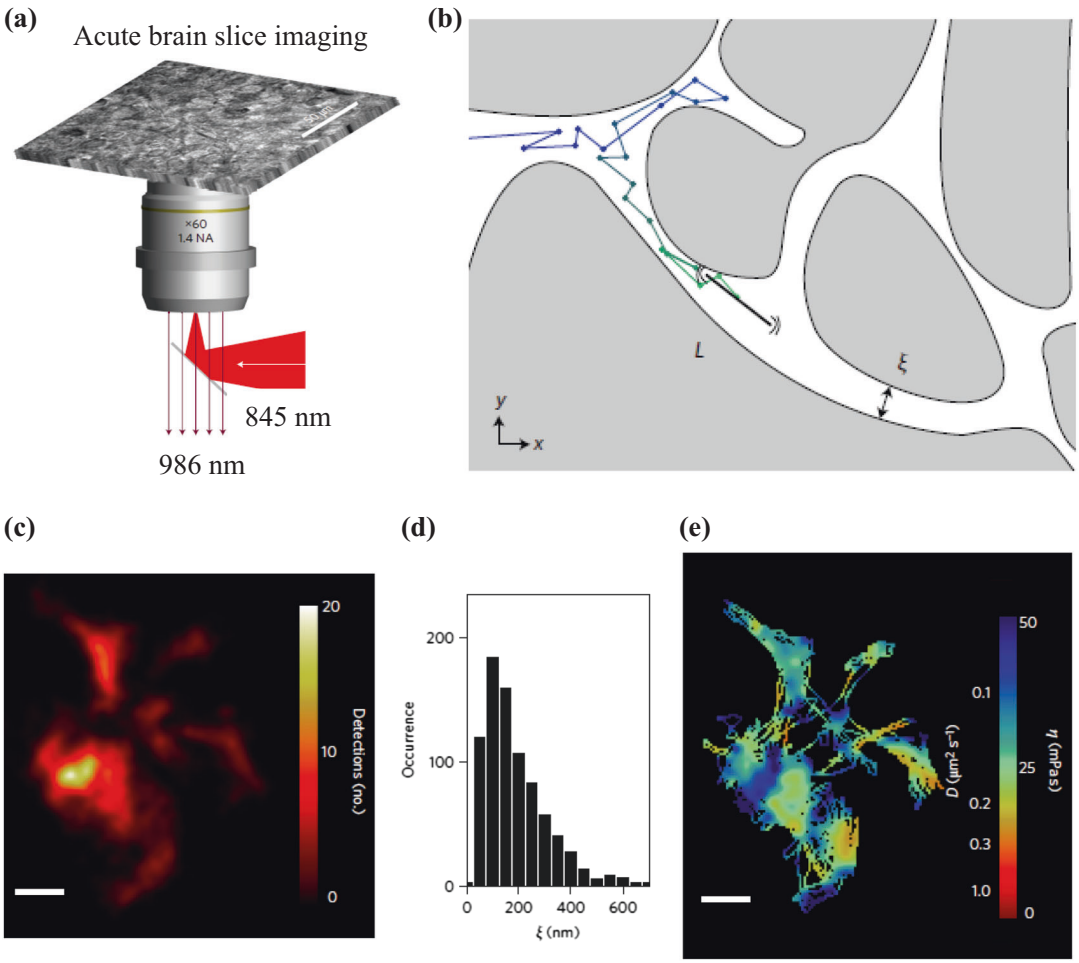

Fig. 8 Individual PLPEG-coated (6,5) SWCNT diffusion properties in the ECS. **a** Luminescent SWCNTs were imaged in brain slices in the NIR range. **b** Schematic representation of an SWCNT of length L diffusing in the ECS. **c** Super-resolved image of the live brain ECS morphology obtained from 20,000 localizations of a diffusing SWCNT. Scale bar, 500 nm. **d** Histogram of ξ ($N = 419$) from 14 super-resolved ECS images as in **c**–**e**. Spatial map of the instantaneous diffusion coefficients of the SWCNTs calculated along the same trajectory using a sliding window of 300 ms. This representation also constitutes a high-resolution spatial map of ECS viscosities (see scale bar). Adopted from ref. [10], Copyright© 2016, Springer Nature

(Fig. 1a). It was feasible to record more than 20,000 images for a single diffusing nanotube in the ECS (Fig. 8b, c). SWCNTs were discovered to be able to travel to many different brain areas, including the neocortex and hippocampus, after only ~30 min of diffusion post injection, indicating that the nanotubes had diffused a relatively long distance from the initial injection sites. Within such a short time, it was possible to travel in only through the ECS [10]. A large population of SWCNTs was found to be trapped by the dead space domains in the brain tissue, suggesting that PLPEG-coated SWCNTs were potentially still sticking to some molecules in the ECS. The typical length of SWCNTs ranged from 490 to 780 nm, and the diameter was ~2–4 nm for PLPEG-coated nanotubes. It is more suitable to consider these SWCNTs as long-aspect-ratio rigid nanometer-scale objects, and their diffusion is mostly unrelated to their flexibility. The distinct diffusion models along two characteristic orientations (along and perpendicular to the nanotubes axis) within a representative timescale of ~200 ms suggest that the nanotubes were confined by their surrounding environment; thus, their movements can be used to study the dynamic structural organization of the ECS. The ECS dimensions were quantitatively calculated, and the width (Fig. 8d) ranged from 80 to 270 nm (150 ± 40 nm, mean ± SD) [10]. These findings indicated that the anisotropic diffusion behavior of single SWCNTs is invaluable for probing the nanometer-scale dimensions of the brain ECS. By fitting the photoluminescence profile of a single nanotube in each image correlated to a time point with a two-dimensional asymmetric Gaussian function, the localization of the nanotube center of mass was extracted at each time point in the imaging plane with a subwavelength accuracy of ~40 nm, and the orientation of the nanotube axis θ relative to the lateral axis in the laboratory frame was

determined (Fig. 1b, inset). SWCNT displacements could then be calculated as the distance traveled by the nanotubes during an observational period. By using a method adopted from single-molecule localization microscopy, a super-resolved image of the ECS was obtained by successively connecting the SWCNT localization positions. This ECS image directly provides information on the spatial, nanometer-scale organization of the live brain ECS. This information suggested that the ECS is a heterogeneous network and contains a number of connected submicrometer domains. These ECS domains were found with typical dimensions ranging from 50 to 700 nm. A super-resolution map of the local ECS viscosity was built based on the lengths of the SWCNTs, and the viscosity ranged from 1 to 50 mPa/s (Fig. 8e), which was approximately two orders of magnitude greater than that of healthy cerebrospinal fluid [10]. These findings indicate that the local viscosity of the ECS is spatially inhomogeneous and that the viscosity values are not directly correlated with the ECS dimensions.

Single-nanotube tracking in live brain tissue was further performed with an animal model created by chemically altering the ECS structure by injecting hyaluronidase into the lateral brain ventricles of young rats. Hyaluronidase dissolved the hyaluronic acids in the ECS and increased the ECS dimensions [10]. As a result, the mean ECS dimensions were 280 ± 60 nm for altered tissue, significantly wider than that of 150 ± 40 nm for native tissue, suggesting that the dissolution of the ECS with hyaluronidase in an inhomogeneous approach to altering local ECS properties. In this study, the ECS dimensions, morphologies, and viscosity revealed by single-nanotube tracking in live brain tissue have provided new insight into the ECS organization down to the nanometer scale.

Conclusion

In summary, reviewed here were some representative achievements in the development of surface-coated SWCNT-based NIR photoluminescence emitters for SPT applications in neuroscience in order to probe complex biological environments, such as the ECS in the live brain. PLPEG-coated SWCNTs have low cytotoxicity compared to nanotubes coated with other surface coating agents based on investigations of cell proliferation, viability, and morphology. PLPEG-coated SWCNTs can be imaged at the single-nanotube level in cell culture, and their nonspecific interactions with live cells were minimal compared to other nanotubes with different coatings. The photoluminescence of single PLPEG-coated SWCNTs is significantly brighter than that of F108-coated nanotubes in cell culture media, allowing video-rate tracking of single nanotubes in biological environments for over several minutes. Three known excitation strategies were carefully compared by considering the impacts of tissue absorption, scattering, and autofluorescence and temperature increases upon excitation at 568 nm for S22, 845 nm for KSB, and 1064 nm for UCL. It is suggested that the 845 nm excitation at the KSB, K-momentum exciton–phonon sideband, is the most suitable for exciting (6,5) PLPEG-coated SWCNTs in order to achieve long-term tracking at a video rate of approximately several tens of Hz in live brain tissue with great imaging depth (≈100 μm) and a high SNR (≈25) without phototoxicity. Finally, it was illustrated that single-nanotube tracking provides a novel approach for revealing the dimensions and viscosity of the ECS at the nanometer scale in the live brain tissue of rats. The ECS was indicated to be a spatial dynamic network of connected polymorphic compartments with nanometer-scale dimensions and specific rheological properties. This information may provide a new understanding of ECS-related cellular communication in brain physiology and pathology.

In the future, three-dimensional tracking of single SWCNTs may be needed to comprehensively understand their diffusion dynamics in natural space and real time in live biological tissue. Biological functionalization of surface-coated SWCNTs with affinity-binding ligands (antibodies, aptamers, and so on) will be useful for utilizing specific targeting biomolecules in vivo and enabling the study of the dynamics of molecules of interest for long-term observation. It is worth noting that PLPEG-coated SWCNTs are capable of efficiently penetrating brain tissue. These nanotubes may be used to establish a novel category of nanometer-sized scaffolds for drug delivery in the brain to treat brain tumors and degenerative diseases.

Compliance with ethical standards

Conflict of interest The authors declare that they have no conflict of interest.

References

1. Rossier O, Octeau V, Sibarita J-B, Leduc C, Tessier B, Nair D, Gatterdam V, Destaing O, Albigès-Rizo C, Tampé R, Cognet L, Choquet D, Lounis B, Giannone G. Integrins β1 and β3 exhibit distinct dynamic nanoscale organizations inside focal adhesions. Nat Cell Biol. 2012;14:1057.
2. Varela JA, Dupuis JP, Etchepare L, Espana A, Cognet L, Groc L. Targeting neurotransmitter receptors with nanoparticles in vivo allows single-molecule tracking in acute brain slices. Nat Commun. 2016;7:10947.
3. Heine M, Groc L, Frischknecht R, Béïque J-C, Lounis B, Rumbaugh G, Huganir RL, Cognet L, Choquet D. Surface mobility of postsynaptic ampars tunes synaptic transmission. Science. 2008;320:201.
4. Petrini EM, Lu J, Cognet L, Lounis B, Ehlers MD, Choquet D. Endocytic trafficking and recycling maintain a pool of mobile

surface ampa receptors required for synaptic potentiation. Neuron. 2009;63:92–105.
5. Biermann B, Sokoll S, Klueva J, Missler M, Wiegert JS, Sibarita JB, Heine M. Imaging of molecular surface dynamics in brain slices using single-particle tracking. Nat Commun. 2014;5:3024.
6. Cognet L, Leduc C, Lounis B. Advances in live-cell single-particle tracking and dynamic super-resolution imaging. Curr Opin Chem Biol. 2014;20:78–85.
7. Gao Z, Danné N, Godin GA, Lounis B, Cognet L. Evaluation of different single-walled carbon nanotube surface coatings for single-particle tracking applications in biological environments. Nanomaterials. 2017;7:393.
8. Akizuki N, Aota S, Mouri S, Matsuda K, Miyauchi Y. Efficient near-infrared up-conversion photoluminescence in carbon nanotubes. Nat Commun. 2015;6:8920.
9. Danné N, Godin AG, Gao Z, Varela JA, Groc L, Lounis B, Cognet L. Comparative analysis of photoluminescence and upconversion emission from individual carbon nanotubes for bioimaging applications. ACS Photonics. 2017;5:359–64.
10. Godin AG, Varela JA, Gao Z, Danné N, Dupuis JP, Lounis B, Groc L, Cognet L. Single-nanotube tracking reveals the nanoscale organization of the extracellular space in the live brain. Nat Nanotechnol. 2016;12:238.
11. Dahan M, Lévi S, Luccardini C, Rostaing P, Riveau B, Triller A. Diffusion dynamics of glycine receptors revealed by single-quantum dot tracking. Science. 2003;302:442.
12. Fakhri N, MacKintosh FC, Lounis B, Cognet L, Pasquali M. Brownian motion of stiff filaments in a crowded environment. Science. 2010;330:1804.
13. Bachilo SM, Strano MS, Kittrell C, Hauge RH, Smalley RE, Weisman RB. Structure-assigned optical spectra of single-walled carbon nanotubes. Science. 2002;298:2361.
14. Cognet L, Tsyboulski DA, Rocha J-DR, Doyle CD, Tour JM, Weisman RB. Stepwise quenching of exciton fluorescence in carbon nanotubes by single-molecule reactions. Science. 2007;316:1465.
15. Welsher K, Liu Z, Sherlock SP, Robinson JT, Chen Z, Daranciang D, Dai H. A route to brightly fluorescent carbon nanotubes for near-infrared imaging in mice. Nat Nanotechnol. 2009;4:773.
16. Heller DA, Jin H, Martinez BM, Patel D, Miller BM, Yeung T-K, Jena PV, Höbartner C, Ha T, Silverman SK, Strano MS. Multimodal optical sensing and analyte specificity using single-walled carbon nanotubes. Nat Nanotechnol. 2008;4:114.
17. Reuel NF, Dupont A, Thouvenin O, Lamb DC, Strano MS. Three-dimensional tracking of carbon nanotubes within living cells. ACS Nano. 2012;6:5420–8.
18. Fakhri N, Wessel AD, Willms C, Pasquali M, Klopfenstein DR, MacKintosh FC, Schmidt CF. High-resolution mapping of intracellular fluctuations using carbon nanotubes. Science. 2014;344:1031.
19. Wang Y, Bahng JH, Che Q, Han J, Kotov NA. Anomalously fast diffusion of targeted carbon nanotubes in cellular spheroids. ACS Nano. 2015;9:8231–8.
20. Zhang X-Q, Xu X, Bertrand N, Pridgen E, Swami A, Farokhzad OC. Interactions of nanomaterials and biological systems: Implications to personalized nanomedicine. Adv Drug Deliv Rev. 2012;64:1363–84.
21. Nel AE, Mädler L, Velegol D, Xia T, Hoek EMV, Somasundaran P, Klaessig F, Castranova V, Thompson M. Understanding biophysicochemical interactions at the nano–bio interface. Nat Mater. 2009;8:543.
22. Zuo G, Kang S-g, Xiu P, Zhao Y, Zhou R. Interactions between proteins and carbon-based nanoparticles: exploring the origin of nanotoxicity at the molecular level. Small. 2013;9:1546–56.
23. Zhao Y, Nalwa HS. Nanotoxicology: interactions of nanomaterials with biological systems. American Scientific Publishers, California, USA, 2007.
24. Duque JG, Cognet L, Parra-Vasquez ANG, Nicholas N, Schmidt HK, Pasquali M. Stable luminescence from individual carbon nanotubes in acidic, basic, and biological environments. J Am Chem Soc. 2008;130:2626–33.
25. Gao Z, Oudjedi L, Faes R, Moroté F, Jaillet C, Poulin P, Lounis B, Cognet L. Optical detection of individual ultra-short carbon nanotubes enables their length characterization down to 10 nm. Sci Rep. 2015;5:17093.
26. Miyauchi Y, Matsuda K, Yamamoto Y, Nakashima N, Kanemitsu Y. Length-dependent photoluminescence lifetimes in single-walled carbon nanotubes. J Phys Chem C. 2010;114:12905–8.
27. Ghosh S, Bachilo SM, Simonette RA, Beckingham KM, Weisman RB. Oxygen doping modifies near-infrared band gaps in fluorescent single-walled carbon nanotubes. Science. 2010;330:1656.
28. Piao Y, Meany B, Powell LR, Valley N, Kwon H, Schatz GC, Wang Y. Brightening of carbon nanotube photoluminescence through the incorporation of sp3 defects. Nat Chem. 2013;5:840.
29. Duque JG, Oudjedi L, Crochet JJ, Tretiak S, Lounis B, Doorn SK, Cognet L. Mechanism of electrolyte-induced brightening in single-wall carbon nanotubes. J Am Chem Soc. 2013;135:3379–82.
30. Duque JG, Pasquali M, Cognet L, Lounis B. Environmental and synthesis-dependent luminescence properties of individual single-walled carbon nanotubes. ACS Nano. 2009;3:2153–6.
31. Wenseleers W, Vlasov II, Goovaerts E, Obraztsova ED, Lobach AS, Bouwen A. Efficient isolation and solubilization of pristine single-walled nanotubes in bile salt micelles. Adv Funct Mater. 2004;14:1105–12.
32. Taranto MP, Fernandez Murga ML, Lorca G, de Valdez GF. Bile salts and cholesterol induce changes in the lipid cell membrane of lactobacillus reuteri. J Appl Microbiol. 2003;95:86–91.
33. Merritt ME, Donaldson JR. Effect of bile salts on the DNA and membrane integrity of enteric bacteria. J Med Microbiol. 2009;58:1533–41.
34. Witus LS, Rocha J-DR, Yuwono VM, Paramonov SE, Weisman RB, Hartgerink JD. Peptides that non-covalently functionalize single-walled carbon nanotubes to give controlled solubility characteristics. J Mater Chem. 2007;17:1909–15.
35. Jakubka F, Schießl SP, Martin S, Englert JM, Hauke F, Hirsch A, Zaumseil J. Effect of polymer molecular weight and solution parameters on selective dispersion of single-walled carbon nanotubes. ACS Macro Lett. 2012;1:815–9.
36. Liu Z, Cai W, He L, Nakayama N, Chen K, Sun X, Chen X, Dai H. In vivo biodistribution and highly efficient tumour targeting of carbon nanotubes in mice. Nat Nanotechnol. 2006;2:47.
37. Cherukuri P, Gannon CJ, Leeuw TK, Schmidt HK, Smalley RE, Curley SA, Weisman RB. Mammalian pharmacokinetics of carbon nanotubes using intrinsic near-infrared fluorescence. Proc Natl Acad Sci USA. 2006;103:18882–6.
38. Chen RJ, Bangsaruntip S, Drouvalakis KA, Wong Shi Kam N, Shim M, Li Y, Kim W, Utz PJ, Dai H. Noncovalent functionalization of carbon nanotubes for highly specific electronic biosensors. Proc Natl Acad Sci USA. 2003;100:4984–9.
39. Moore VC, Strano MS, Haroz EH, Hauge RH, Smalley RE, Schmidt J, Talmon Y. Individually suspended single-walled carbon nanotubes in various surfactants. Nano Lett. 2003;3:1379–82.
40. Gao Z, Varela JA, Groc L, Lounis B, Cognet L. Toward the suppression of cellular toxicity from single-walled carbon nanotubes. Biomater Sci. 2016;4:230–44.
41. Liu Z, Davis C, Cai W, He L, Chen X, Dai H. Circulation and long-term fate of functionalized, biocompatible single-walled carbon nanotubes in mice probed by raman spectroscopy. Proc Natl Acad Sci USA. 2008;105:1410–5.
42. Wang X, Xia T, Duch MC, Ji Z, Zhang H, Li R, Sun B, Lin S, Meng H, Liao Y-P, Wang M, Song T-B, Yang Y, Hersam MC, Nel AE. Pluronic f108 coating decreases the lung fibrosis potential

of multiwall carbon nanotubes by reducing lysosomal injury. Nano Lett. 2012;12:3050–61.
43. Ge C, Du J, Zhao L, Wang L, Liu Y, Li D, Yang Y, Zhou R, Zhao Y, Chai Z, Chen C. Binding of blood proteins to carbon nanotubes reduces cytotoxicity. Proc Natl Acad Sci USA. 2011;108:16968–73.
44. Määttä J, Vierros S, Van Tassel PR, Sammalkorpi M. Size-selective, noncovalent dispersion of carbon nanotubes by pegylated lipids: a coarse-grained molecular dynamics study. J Chem Eng Data. 2014;59:3080–9.
45. Määttä J, Vierros S, Sammalkorpi M. Controlling carbon-nanotube—phospholipid solubility by curvature-dependent self-assembly. J Phys Chem B. 2015;119:4020–32.
46. Lee H. Molecular dynamics studies of pegylated single-walled carbon nanotubes: the effect of peg size and grafting density. J Phys Chem C. 2013;117:26334–41.
47. Liu X, Tao H, Yang K, Zhang S, Lee S-T, Liu Z. Optimization of surface chemistry on single-walled carbon nanotubes for in vivo photothermal ablation of tumors. Biomaterials. 2011;32:144–51.
48. Sacchetti C, Motamedchaboki K, Magrini A, Palmieri G, Mattei M, Bernardini S, Rosato N, Bottini N, Bottini M. Surface polyethylene glycol conformation influences the protein corona of polyethylene glycol-modified single-walled carbon nanotubes: potential implications on biological performance. ACS Nano. 2013;7:1974–89.
49. Bisker G, Dong J, Park HD, Iverson NM, Ahn J, Nelson JT, Landry MP, Kruss S, Strano MS. Protein-targeted corona phase molecular recognition. Nat Commun. 2016;7:10241.
50. Ritz S, Schöttler S, Kotman N, Baier G, Musyanovych A, Kuharev J, Landfester K, Schild H, Jahn O, Tenzer S, Mailänder V. Protein corona of nanoparticles: distinct proteins regulate the cellular uptake. Biomacromolecules. 2015;16:1311–21.
51. Obst K, Yealland G, Balzus B, Miceli E, Dimde M, Weise C, Eravci M, Bodmeier R, Haag R, Calderón M, Charbaji N, Hedtrich S. Protein corona formation on colloidal polymeric nanoparticles and polymeric nanogels: Impact on cellular uptake, toxicity, immunogenicity, and drug release properties. Biomacromolecules. 2017;18:1762–71.
52. Godin AntoineG, Lounis B, Cognet L. Super-resolution microscopy approaches for live cell imaging. Biophys J. 2014;107:1777–84.
53. Diao S, Hong G, Antaris AL, Blackburn JL, Cheng K, Cheng Z, Dai H. Biological imaging without autofluorescence in the second near-infrared region. Nano Res. 2015;8:3027–34.
54. Roxbury D, Jena PV, Williams RM, Enyedi B, Niethammer P, Marcet S, Verhaegen M, Blais-Ouellette S, Heller DA. Hyperspectral microscopy of near-infrared fluorescence enables 17-chirality carbon nanotube imaging. Sci Rep. 2015;5:14167.
55. Oudjedi L, Parra-Vasquez ANG, Godin AG, Cognet L, Lounis B. Metrological investigation of the (6,5) carbon nanotube absorption cross section. J Phys Chem Lett. 2013;4:1460–4.
56. Antaris AL, Robinson JT, Yaghi OK, Hong G, Diao S, Luong R, Dai H. Ultra-low doses of chirality sorted (6,5) carbon nanotubes for simultaneous tumor imaging and photothermal therapy. ACS Nano. 2013;7:3644–52.
57. Santos SM, Yuma B, Berciaud S, Shaver J, Gallart M, Gilliot P, Cognet L, Lounis B. All-optical trion generation in single-walled carbon nanotubes. Phys Rev Lett. 2011;107:187401.
58. Steven LJ. Optical properties of biological tissues: a review. Phys Med Biol. 2013;58:R37.
59. Syková E, Nicholson C. Diffusion in brain extracellular space. Physiol Rev. 2008;88:1277–340.
60. Nicholson C, Chen KC, Hrabětová S, Tao L. Diffusion of molecules in brain extracellular space: theory and experiment. In: Agnati LF, Fuxe K, Nicholson C, Sykova E, editors. Progress in brain research. Amsterdam: Elsevier; 2000.
61. Nicholson C, Kamali-Zare P, Tao L. Brain extracellular space as a diffusion barrier. Comput Vis Sci. 2011;14:309–25.
62. Dityatev A, Schachner M, Sonderegger P. The dual role of the extracellular matrix in synaptic plasticity and homeostasis. Nat Rev Neurosci. 2010;11:735.
63. Xie L, Kang H, Xu Q, Chen MJ, Liao Y, Thiyagarajan M, O'Donnell J, Christensen DJ, Nicholson C, Iliff JJ, Takano T, Deane R, Nedergaard M. Sleep drives metabolite clearance from the adult brain. Science. 2013;342:373–7.
64. Metzler-Baddeley C, Jones DK, Belaroussi B, Aggleton JP, O'Sullivan MJ. Frontotemporal connections in episodic memory and aging: a diffusion mri tractography study. J Neurosci. 2011;31:13236–45.
65. Lehmenkühler A, Syková E, Svoboda J, Zilles K, Nicholson C. Extracellular space parameters in the rat neocortex and subcortical white matter during postnatal development determined by diffusion analysis. Neuroscience. 1993;55:339–51.
66. Verkman AS. Diffusion in the extracellular space in brain and tumors. Phys Biol. 2013;10:045003.
67. Ohno N, Terada N, Saitoh S, Ohno S. Extracellular space in mouse cerebellar cortex revealed by in vivo cryotechnique. J Comp Neurol. 2007;505:292–301.
68. Korogod N, Petersen CCH, Knott GW. Ultrastructural analysis of adult mouse neocortex comparing aldehyde perfusion with cryo fixation. eLife. 2015;4:e05793.